Experimental Set-up for Applying Wind Turbine Operating Profiles to the Nacelle Power Converter

C.J. Smith[#1], C.J. Crabtree[#], P.C. Matthews[#]

[#]*School of Engineering and Computing Sciences, Durham University*

Lower Mountjoy, South Road, Durham, DH1 3LE, UK

[1]c.j.smith2@dur.ac.uk

Abstract – **Studies have shown that the reliability of fully rated converters (FRC) in permanent magnet synchronous generator (PMSG) wind turbines is critical. This paper outlines an experimental rig that applies PMSG wind turbine specific operating profiles to a machine side converter (MSC) power module. A number of test regimes have been designed to verify thermal models of the power module, validate the use of cycle life vs. T_j profile manufacturing data, and determine the wind turbine operational profiles that cause the most damage to the MSC.**

Keywords – Experimental set-up, PMSG Power Converter, Reliability, Operating Profiles

I. INTRODUCTION

To meet EU renewable energy targets for 2020 and beyond, the Levelised Cost of Energy (LCoE) of offshore wind needs to be reduced from the current £140/MWh to below £100/MWh [1]. Operation and maintenance costs account for around 30% of the LCoE [2] and therefore research has focused on understanding the reliability of components and their impact on the LCoE.

Carroll et al [3] examined a large dataset for offshore wind turbines with varying turbine technology to determine the main causes of failure and concluded that the power converter had a typical failure rate of ~0.2 failures/turbine/year (f/t/y) over the turbine population. However, a more focused study on turbine type [4] found that the failure rate of fully-rated converters (FRC) in permanent magnet synchronous generator (PMSG) turbines was 0.593 f/t/y compared to the 0.106 f/t/y for doubly fed induction generator (DFIG) turbines. Of these failures, power module failure is the failure mode for nearly all major converter repairs. FRC reliability is critical for PMSG turbines, with power module failure the dominant failure mode.

Typically, power module failures are linked to the thermal loading of the devices. In literature this has been tested using cycles-to-failure against insulated gate bipolar transistor (IGBT) junction temperature swing (ΔT_j) data [5]. However, whilst power module failure modes are well understood, manufacturing failure data is often produced at fixed ΔT_j [6], implying a fixed current operating profile. This is not representative of wind turbine converter operation as the variable wind speed produces a variable current throughput of the converter. Therefore harmful operating conditions may have their impact on reliability omitted. There is a need to explore the impact of realistic PMSG wind turbine operation on the FRC's reliability. Therefore the following research questions were formulated:

- Are the thermal loading profiles generated in the power modules verifiable?
- Which wind speed operating conditions cause the greatest thermal loading to the power modules in the power converter and does this correspond to the greatest damage?
- Is manufacturing thermal data a valid approach for lifetime estimation under complex loading conditions such as operation in a wind turbine?

To address these research questions an experimental rig is being designed and constructed which will subject a test bench machine-side converter (MSC) to operating conditions from a PMSG wind turbine. The rig will provide both physical testing and verification of existing power module thermal models. This paper details the outline of this rig and how the research questions will be answered.

The paper is organised as follows. Section II outlines the experimental set up, Section III details the experiments which will be carried out to answer the research questions and Section IV summarises the details of the paper.

II. METHODOLOGY

This section outlines the key aspects of the experimental rig which emulates a PMSG turbine electrical drive train. Fig.1 shows a schematic diagram of the experimental rig.
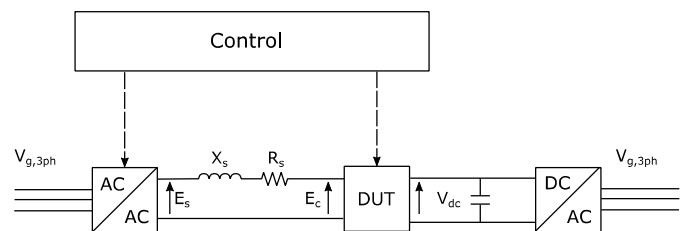

Fig. 1: Circuit diagram of experimental rig. V_g is the grid voltage, E_a is the simulated generator armature voltage, X_s is the stator reactance, R_s is the stator resistance, E_c is the converter voltage and V_{dc} is the DC-link voltage.

An AC power supply will be controlled to apply wind turbine specific operational profiles on a device under test (DUT). This DUT is the MSC of the turbine drive train and is switched to convert the AC input to DC. This DC output feeds a DC link which acts as the grid-side converter (GSC) in the turbine, sinking the power back to the grid. The rest of this section gives details on key aspects of the experimental rig.

A. AC power supply

This section details the emulation of a PMSG and mechanical drive train using an AC power supply and impedance.

Typically wind turbine drive train experimental rigs emulate the mechanical components of the turbine that connect to the generator (blades, hub, drive shaft etc.) using a controlled motor mechanically coupled to the generator [7, 8]. Whilst this ensures accurate generator output, the machine characteristics that can be emulated are limited to the generators available at the rig power rating, or require a unique design request. As PMSGs constructed for direct-drive turbines have a large number of pole pairs, finding a suitable scaled version for the rig power rating can be difficult. This also limits the range of machine parameters available for testing. It was deemed that another solution was required.

To allow for the emulation of PMSGs used in present and future wind turbines the generator and mechanical coupling is replaced by a controllable AC voltage supply and phase impedance (Fig. 2). The AC supply emulates the PMSG's armature voltage (E_a). The phase impedance includes a known inductance and resistance to emulate the stator impedance that defines the machine characteristics. The AC supply is controllable so that the E_a responds to the turbine speed. The speed is based on the wind conditions, converter voltage (E_c) and drive train dynamics as simulated in [9]. The AC supply and impedance set-up allows for a wide range of PMSG parameters to be emulated by changing the impedance and the control of the AC power supply.
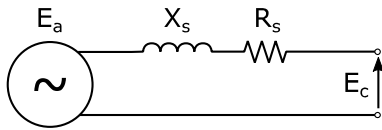

Fig. 2: Synchronous generator armature per-phase circuit diagram. X_s is the stator reactance and R_s is the stator resistance.

This set-up has a number of advantages. As mentioned, the emulated machine characterises are not limited by the available generators. The rig is also flexible to explore the impact of slight variations in generator design and can be modified to emulate other generator types. The loss of mechanical emulation also simplifies the construction and control of the rig. Therefore the use of an AC power supply as a replacement for the typical mechanical set-up allows for a simpler and more flexible experimental rig.

The mechanical components and PMSG of the wind turbine are emulated using a controllable AC power supply and impedances.

B. DUT

This section outlines the choice of converter topology and power module for testing in the experimental rig. Fig. 3 gives the circuit diagram of the DUT. The boxes indicate the devices of interest; the red box is an IGBT and the blue box is a diode.

In the simulations in previous work [10] two parallel SEMIKRON SKSB1090GD69/11-MAPB stacks [11] were used for the MSC. These stacks contained the SKiiP1513GB172-3DWV3 half-bridge SKiiP module [12] for each leg in the stacks. Ideally these modules would be the DUTs but this was impractical due to the indicative cost, current and voltage rating (1500A$_{nom}$ and 1700V$_{ces}$) of these SKiiP modules. Therefore a lower rated power module was required for the DUT.
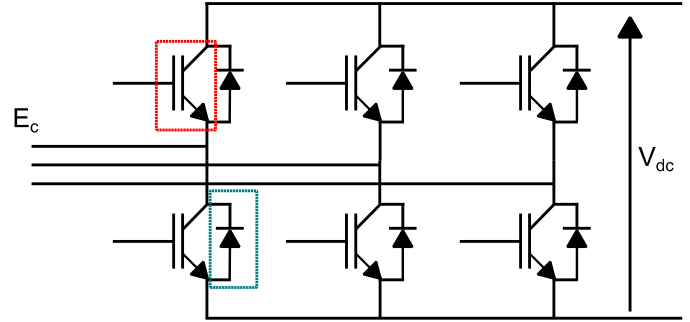

Fig. 3: Circuit diagram of the DUT. The DUT is a full-bridge rectifier.

The lower rated power module used for the rig is the SEMIKRON 11NAB066V1 MiniSKiiP module [13]. This module has a much lower current and voltage rating (6A$_{nom}$ and 600V$_{ces}$) and much lower unit cost. This allows for practical laboratory testing to failure. The module contains a 3-phase rectifier and inverter but can be reconfigured to only use the rectifier. It has been assumed that the separate legs of the converter are thermally isolated, as found in [8], which will be verified during commissioning.

The key limitation of using the 11NAB066V1 module is that the packaging technology differs from the SKiiP1513 module. For example the SKiiP1513 uses SKiNTER technology which replaces solder with cold welded silver between direct bonded copper (DCB) and chip [14]. However, according to expert advice, this only increases the lifetime of the device and does not change the fundamental failure mode. Therefore the 11NAB066V1 module was deemed suitable for emulation of the large modules found in MW-scale turbines.

To summarise, the 11NAB066V1 MiniSKiiP module was chosen as the DUT as it has current and voltage ratings that allow for practical laboratory testing and it has the same IGBT technology as the larger SKiiP modules found in MW-scale wind turbines.

C. DC Link

This section outlines the rationale for using a constant voltage source for the DC link.

In a typical wind turbine the converter is comprised of back-to-back rectifier/inverter. The rectifier acts as the MSC and the inverter acts as the GSC. The role of the MSC and GSC differs depending on control strategy but the MSC typically controls the speed of the wind turbine for optimum power production whilst the GSC maintains the DC link voltage. Due to turbine speed variation the MSC experiences a more varied operating profile compared to the fixed frequency GSC. The MSC is consequently of greater interest for reliability analysis. Therefore, only the MSC is used as a DUT and the GSC is replaced with a constant voltage source to maintain the DC link.

As the DUT collector-emitter saturation voltage (V_{ces}) is lower than MW-scale power modules, the DC link voltage must be scaled accordingly. In order to maintain consistency in terms of reliability, Eq. (1) can be applied to determine the equivalent DC link voltage.

$$V_{dc,e} = V_{ces,e} \frac{V_{dc,f}}{V_{ces,f}} \qquad (1)$$

where $V_{dc,e}$ and $V_{dc,f}$ are the experimental and full-scale DC link voltage respectively, and $V_{ces,e}$ and $V_{ces,f}$ are the experimental and full-scale power module collector-emitter saturation voltage respectively.

To summarise, the GSC of a typical turbine has been replaced with an ideal DC link voltage in the experimental rig. The value of the DC link voltage is determined using the ratio between the V_{ces} of the full-scale and the DUT.

D. Control

There are two main aspects of control in the experimental rig: control of the AC power supply and control of the DUT switching.

The AC power supply will be controlled to emulate the variation in E_a due to the speed change of the turbine. This E_a variation will depend on the wind speed operational profile that is produced for the given test (Section III), and will be calculated using the drive train model detailed in [9]. The rig will be pre-programmed with the E_a profile for testing.

The DUT is switched to produce a desired E_c. For this work the control strategy chosen was vector control as it can reach steady state after a turbine speed variation faster than load angle control [15]. The switching strategy used is sine wave pulse width modulation (SPWM), but space-vector PWM (SVPWM) is also available due to the flexibility built into the DC link voltage. In summary the DUT is switched using SPWM and the E_c is calculated to provide vector control.

The two rig components that are controlled are the AC power supply and DUT. These are controlled to provide the required E_a and E_c, with E_a determined by a drive train model and E_c determined by the implemented vector control. The DUT's IGBT switching pattern is determined by SPWM.

E. Measurement Strategy

In order to provide the information needed to answer the research questions in Section I a measurement strategy is required. Three main measurements were deemed crucial:

- High frequency current measurement to determine current passing through devices (Q1, 2).
- High frequency, high quality temperature measurements at points in the power module to verify T_j data and provide reference thermal loading for lifetime estimation (Q1-3).
- High quality images of power modules to determine where damage has occurred or is accumulating (Q2, 3).

The provision of high frequency current measurement requires current transducers and data acquisition that are able to take measurements at approximately 20kHz (20kS/s). These devices are widely available.

The temperature measurement is more complex. Due to the size of the power modules placing thermocouples in important areas e.g. the IGBT junction, will require precision placement and is unlikely to provide accurate high frequency measurements. Instead, a thermal imaging approach will be taken. This will require removal of the module casing but will provide a higher fidelity picture of the thermal loading on the device. These images can also be taken at high frequency and analysed to provide temperature profiles. Therefore a thermal imaging camera will be used for temperature measurement.

The use of high quality images of the device will allow for optical inspection of the DUT for damage accumulation or finding root cause of failure. Damage accumulation will be mapped by taking the DUT out of the rig and inspecting for damage at regular intervals. These high quality images can be created using a suitable microscope.

The measurement strategy to answer the 3 research questions will include current measurement, thermal imaging and regular inspection for damage accumulation and failure mode using a microscope.

F. Summary

The experimental rig consists of the following key components:

- A controllable AC power supply with selected impedance to emulate the mechanical drive train and generator.
- The DUT MSC is the 11NAB066V1 MiniSKiiP module and is used in vector control mode with SPWM.
- The GSC has been replaced with an ideal DC link voltage and feeds power back to the grid.
- The measurements taken will include current in the power modules, thermal imaging to determine T_j and regular optical inspection for damage accumulation and failure mode using a microscope.

III. PLANNED TESTING

This section details the testing regimes that will be applied to the experimental rig in order to answer the 3 research questions detailed in Section I.

A. Thermal Loading Verification

The verification of the work done in [10] is a key first step. This will determine how well T_j can be predicted given the current throughput of the device. This is an important first step in determining whether the current history of a device can be used to predict the remaining life of the module.

This verification will be done by applying known current profiles to the device and waiting for the device to reach steady state. The T_j will be compared to simulated T_j profiles. Fig 4 gives examples of some simulated T_j profiles at various wind speeds.
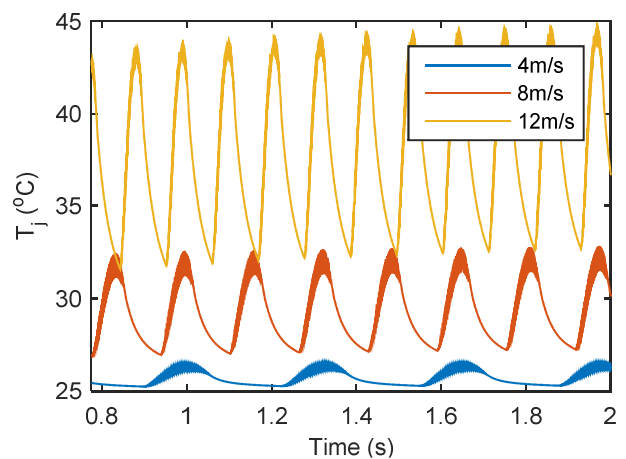

Fig. 4: Example of simulated T_j profiles at various wind speeds.

B. Determining Operating Conditions That Cause Greatest Thermal Loading

One of the outputs of this work is to determine if particular operating profiles can be linked to particular thermal loading patterns on the DUT. To do this, specific wind characteristics

will be isolated (Fig. 5) and simulated using the approach in [10]. The profiles found to have the highest simulated T_j loading profiles will be emulated and applied to the DUT and the results verified. The damage accumulated on the DUT will then be monitored to validate whether higher T_j causes accelerated failure as suggested by manufacturing data.
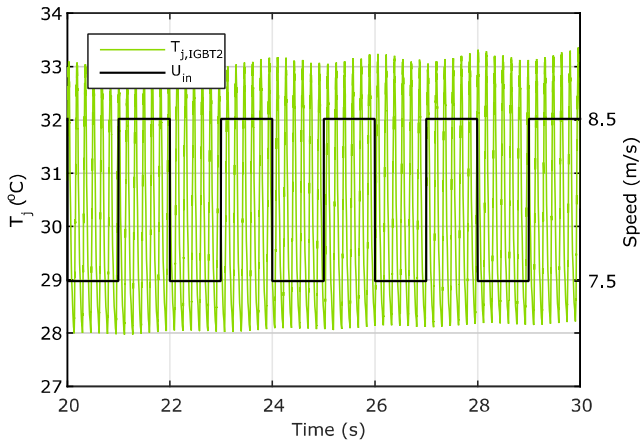

Fig. 5: Example of controlled wind speed input condition. The $T_{j,IGBT2}$ is the simulated T_j profile on an IGBT in the power module.

C. Validation of Lifetime against Thermal Loading Concept

To validate the cycles-to-failure concept an operational profile will be applied to the drive train simulation. The resultant simulated T_j will be used with manufacturing data to produce an expected end of life for the device. The profile will then be applied to the DUT until failure and the lifetime compared to the predicted lifetime.

As this experiment requires a large run time, to speed up the process the profile will be designed to include the most potentially damaging conditions found from experiments in Section III.B. The optical inspection of the device will also be closely examined to monitor signs of damage.

D. Summary

The research questions will be answered by applying test regimes to the experimental rig. These test regimes are:

- Thermal loading verification by applying a known current profile and comparing the resultant T_j profile with the simulated T_j profile.
- Determining potentially harmful operating conditions by determining profiles that cause the highest thermal loading, applying the profile to the test rig and monitoring the damage to the device.
- Validation of cycle life against T_j profile concept by applying a theoretically abusive operating profile and comparing expected and actual lifetime of the DUT.

IV. CONCLUSION

Operation and maintenance accounts for around 30% of the LCoE of offshore wind turbines and therefore research has focused on understanding the reliability of turbine components. Studies have shown that the FRC in PMSG wind turbines is critical for reliable operation of the wind turbine. Therefore there is a need to explore the impact of realistic PMSG wind turbine operation on the FRC's reliability. In response three research questions were outlined that aim to explore the causes of converter failure in PMSGs with a focus on thermal loading of the converter power modules.

This paper has outlined an experimental rig that aims to answer these research questions by applying PMSG wind turbine specific operating profiles to a MSC power module. One of the key features is the replacement of the typical motor-generator coupling with a more flexible controllable AC power supply with selected impedance to emulate the mechanical drive train and generator.

The research questions will be answered by applying test regimes to the experimental rig. These test regimes compare simulated T_j profiles and expected device lifetimes with physical testing results to verify thermal models, validate the use of T_j profile against cycle life data, and determine the operational profiles that cause the most damage to the MSC.

V. REFERENCES

[1] E. Davey and A. Nimmo. (2012). *Offshore Wind Cost Reduction, Pathways Study*. Available: http://www.thecrownestate.co.uk/media/305094/offshore-wind-cost-reduction-pathways-study.pdf

[2] W. Musial and B. Ram. (2010). *Large-Scale Offshore Wind Power in the United States: Assessment of Opportunities and Barriers*. Available: http://www.nrel.gov/docs/fy10osti/40745.pdf

[3] J. Carroll, A. McDonald, and D. McMillan, "Failure rate, repair time and unscheduled O&M cost analysis of offshore wind turbines," *Wind Energy,* 2015.

[4] J. Carroll, A. McDonald, and D. McMillan, "Reliability Comparison of Wind Turbines With DFIG and PMG Drive Trains," *IEEE Transactions on Energy Conversion,* vol. 30, p. 663, 2015.

[5] K. Ma, M. Liserre, F. Blaabjerg, and T. Kerekes, "Thermal loading and lifetime estimation for power device considering mission profiles in wind power converter," *IEEE Transactions on Power Electronics,* vol. 30, pp. 590-602, 2015.

[6] ABB. (2014). *Load-cycling capability of HiPak IGBT modules*. Available: https://library.e.abb.com/public/1f4fb71e0af3356883257c8d00443ca1/Load-cycling%20capability%20of%20HiPak_5SYA%202043-04.pdf

[7] S. Djurovic, C. J. Crabtree, P. J. Tavner, and A. Smith, "Condition monitoring of wind turbine induction generators with rotor electrical asymmetry," *IET Renewable Power Generation,* vol. 6, pp. 207-216, 2012.

[8] P. Wyllie, "Electrothermal Modelling for Doubly Fed Induction Generator Converter Reliability in Wind Power," Durham University Thesis, 2014.

[9] C. J. Smith, C. J. Crabtree, and P. C. Matthews, "Characterisation of Electrical Loading Experienced by a Wind Turbine Power Converter (under review)," presented at the EWEA Annual Event Paris, France, 2015.

[10] C. J. Smith, C. J. Crabtree, and P. C. Matthews, "Impact of wind conditions on thermal loading of PMSG wind turbine power converter (under review)," in *8th IET International Conference on Power Electronics, Machines and Drives*, Glasgow, UK, 2016.

[11] SEMIKRON. (2013). *SKS B1 090 GD 69/11 - MA PB Datasheet*. Available: http://www.semikron.com/dl/service-support/downloads/download/semikron-datasheet-sks-b1-090-gd-69-11-ma-pb-08800136

[12] SEMIKRON. (2014). *SKiiP 1513 GB172-3DW V3 Datasheet*. Available: http://www.semikron.com/dl/service-support/downloads/download/semikron-datasheet-skiip-1513-gb172-3dw-v3-20451120

[13] SEMIKRON. (2006). *SKiiP 11NAB066V1 Datasheet*. Available: http://www.semikron.com/dl/service-support/downloads/download/semikron-datasheet-skiip-11nab066v1-25230580

[14] SEMIKRON. (2015). *SKiNTER Technology*. Available: http://www.semikron.com/innovation-technology/construction-and-connection-technology/skinter-technology.html

[15] O. Anaya-Lara, N. Jenkins, J. Ekanayake, P. Cartwright, and M. Hughes, *Wind energy generation: modelling and control*: John Wiley & Sons, 2011.